Photoinduced Volume Changes in Amorphous Selenium

J. Hegedüs,[1] K. Kohary,[2] D. G. Pettifor,[2] K. Shimakawa,[3] and S. Kugler[4]

[1]*Department of Physics and Material Sciences Center, Philipps University Marburg, Renthof 5, D-35032 Marburg, Germany*
[2]*Department of Materials, University of Oxford, Parks Road, Oxford, OX1 3PH, United Kingdom*
[3]*Department of Electrical and Electronic Engineering, Gifu University, Gifu 501-1193, Japan*
[4]*Department of Theoretical Physics, Budapest University of Technology and Economics, H-1521 Budapest, Hungary*

(Received 3 June 2005; published 8 November 2005)

We have modeled the photoinduced volume change in amorphous selenium. After photon absorption, we treated the excited electron and hole independently within the framework of the tight-binding formalism. We found covalent bond breaking in amorphous networks with photoinduced excited electrons, whereas excited holes contribute to the formation of interchain bonds. We also observed a correlated volume change of the amorphous samples. Our results provide a new and universal description, which can simultaneously explain the photoinduced volume expansion and shrinkage. This model is supported by very recent *in situ* surface height measurements for amorphous selenium.

DOI: 10.1103/PhysRevLett.95.206803 PACS numbers: 73.61.Jc, 71.55.Jv

During band gap illumination, chalcogenide glasses exhibit various changes in structural and electronic properties such as photoinduced volume change, photodarkening, defect creation, and photoinduced change in the phase state. These phenomena are unique to chalcogenide glasses, and they are not observed in the crystalline chalcogenides nor in any other amorphous semiconductors. The changes are facilitated by factors common to chalcogenide glasses: the low average coordination number and the structural freedom of the noncrystalline state. Materials showing photoinduced volume change can be classified into two different groups: Films can either expand (a-As_2S_3, a-As_2Se_3, etc.) or shrink (a-$GeSe_2$, a-$GeSe_2$, etc.) [1]. Several investigations have been carried out in order to provide an explanation of the photoinduced phenomena [2–7]. It has been established that there is a configurational rearrangement with changes in atomic coordination in the vicinity of the excitation [4–6]. In a simplistic model, such changes in the local bonding environment were explained by the formation of valence alteration pairs (pair of coordination defects) [4]. In selenium, formation of new interchain bonds was also suggested [5]. However, an atomistic study for amorphous selenium has revealed that structural rearrangements are less local than in such simple models and has given evidence that further possible bond formations and bond breakings are responsible for photoinduced effects [6]. A cumulative effect of these changes in local configuration is expected to be responsible for the macroscopic effects, but an acceptable general theory which can simultaneously describe photoinduced expansion and shrinkage in amorphous chalcogenides is still missing. In this Letter, we propose a simple, unified description of the photoinduced volume changes in chalcogenides based on tight-binding (TB) molecular dynamics (MD) simulations of amorphous selenium. We found that microscopic rearrangements in the structure (such as bond breaking and bond formation) are responsible for the macroscopic volume change under illumination. The first *in situ* surface height measurement [8] on amorphous selenium was carried out recently and supports our proposed mechanism.

The photoinduced volume changes were simulated using our TB-MD computer code ATOMDEP, which has modeled both amorphous carbon [9] and amorphous silicon [10]. For the description of interatomic interactions between selenium atoms, we have used the TB model developed by Molina *et al.* [11]. Self-consistency was taken into account via the usual on-site Hubbard term and was found to reduce any large charge transfer [12]. We used the velocity Verlet algorithm to follow the motion of atoms with a time step equal to $\Delta t = 2$ fs. The temperature was controlled via the velocity-rescaling method.

Thirty different glassy selenium networks were prepared in a rectangular box with periodic boundary conditions. Samples contained 162 atoms, and the size of our initial simulation cell was 12.78 Å $\times$ 12.96 Å $\times$ 29.69 Å (xyz). Our ''cook and quench'' sample preparation procedure was the following. First, we chose the temperature of the system to be 5000 K for the first 300 MD steps to randomize the atomic positions by melting the samples. During the following 2200 MD steps, we decreased the temperature linearly from 700 to 250 K, driving the sample through the glass transition and reaching the condensed phase. Then we set the final temperature to 20 K and we relaxed the sample for 500 MD steps (1 ps). In order to model the photoinduced volume changes, the periodic boundary conditions were lifted along the z direction at this point. This procedure provided us a slab geometry with periodic boundary conditions in only two dimensions. The system was then relaxed for another 40 000 MD steps (80 ps) at $T = 20$ K. Short quenching times in the simulation compared to those in the experiments might lead to many liquid-state defects being retained in the amorphous structure. Therefore, the Hubbard parameter U was taken as

5 eV for the first 4000 MD steps during quenching in order to avoid a large number of coordination defects, especially onefold C_1 and threefold C_3 coordinated atoms. Then we changed U to its accepted value of 0.875 eV for selenium [12].

The radial distribution function for one of our selenium glassy networks at 20 K is shown in Fig. 1. The first peak at 2.4 Å belongs to covalently bonded atoms, being close to the crystalline nearest-neighbor distance of 2.37 Å. The second peak at 3.6 Å corresponds to the intrachain second nearest-neighbor distance. The prepeak at 3.3 Å reflects the smallest interchain atomic distances in amorphous selenium. In simulations at larger temperatures ($T = 300$ K), these two peaks merge, as observed in Fig. 1.

Photoexcitations generate electron-hole pairs. We model this process by transferring an electron from the highest occupied molecular orbital (HOMO) to the lowest unoccupied molecular orbital (LUMO) when a photon is absorbed. This technique was first applied to describe the photoinduced effects in eight-member sulfur rings within the framework of density functional theory [13]. We used a similar method to test the photoinduced changes in different selenium clusters, such as an 8-member ring and an 18-member linear chain. We observed photoinduced bond breaking inside these selenium clusters similarly to the case of sulfur [13].

In our simulations, we assumed that immediately after photon absorption the electron and the hole became separated in space on a femtosecond time scale, so that we could treat them independently [14]. We neglect the effective Columb interaction between the electron and hole, and, therefore, we ran two sets of simulations: First, we put an extra electron into the LUMO (excited electron creation), and, second, we annihilated an electron in the HOMO (hole creation). When an additional electron was put in the LUMO, a bond-breaking event occurred, as expected. In the majority of cases, a covalent bond between twofold- and threefold-coordinated atoms was broken ($C_2 + C_3 \Rightarrow C_1 + C_2$), as illustrated schematically in Fig. 2. Our localization analysis revealed that the LUMOs were usually localized at such sites before bond breaking, as observed in Fig. 2. The bond breaking significantly affects the bond lengths, which alternates between shrinkage and elongation in the vicinity of the broken bond, as seen in Fig. 2. If the electron on the LUMO is deexcited, then we observed that all the bond lengths are restored to their original value.

The time development of a particular photoinduced bond-breaking event is shown in Fig. 3, which is characteristic for similar changes we observed during other bond-breaking events. Before the excitation at 5 ps, the bond has a length of about 2.55 Å, corresponding to a bond between a twofold- and a threefold-coordinated atom, as illustrated in Fig. 2. This bond is weaker and has an interatomic separation larger than the 2.4 Å of the majority of nearest-neighbor bonds between twofold-coordinated sites. During illumination, this weak bond increases by 10%–20%, decreasing to its original value after deexcitation of the electron at 15 ps. We measured the corresponding volume change by calculating the variation in thickness of our amorphous selenium slab. The volume change follows the bond breaking, and it shows damped oscillations on the picosecond time scale, as seen in Fig. 3.

In contrast, a very different behavior was observed during hole creation, in that interchain bonds are formed after creating a hole, thereby causing the contraction of the sample, as observed in Fig. 4. This always happens near the atoms where the HOMO is localized. Since the HOMO is usually localized in the vicinity of a onefold-coordinated atom, the interchain bond formation often takes place between a onefold-coordinated atom and a twofold-coordinated atom ($C_{1,0} + C_{2,0} \Rightarrow C_{1,1} + C_{2,1}$, where the second subscript means the number of interchain bonds).

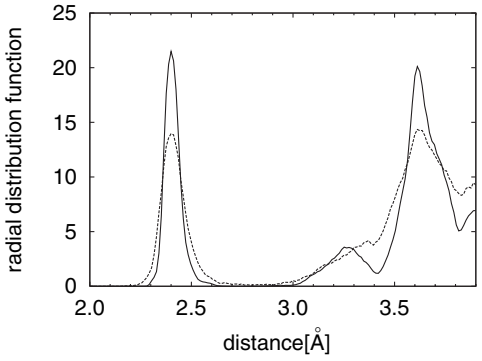

FIG. 1. Radial distribution function of selenium glassy networks at $T = 20$ K (solid line) and at $T = 300$ K (dashed line). First peak at 2.4 Å belongs to covalently bonded atoms. Second peak at 3.6 Å corresponds to intrachain second nearest-neighbor distance. Prepeak around 3.3 Å represents distances between two atoms in two different chains (interchain bond). These two peaks merge at larger temperature ($T = 300$ K).

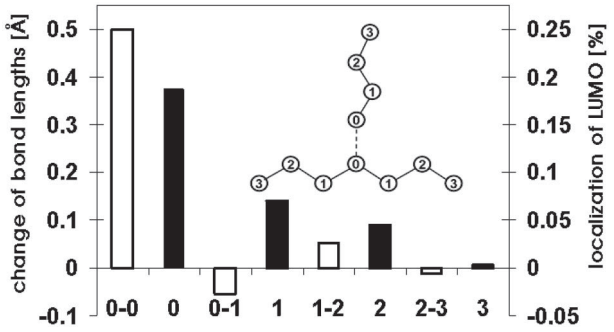

FIG. 2. Average change of bond lengths (open bars) and average localization of LUMO (solid bars) on atoms in the vicinity of bond breaking, which is also shown schematically. LUMO is localized at a bond-breaking site (atoms "0," "1," "2"). Photoinduced breaking bond ("0-0") causes alternation of bond shrinkage and elongation of further bonds ("0-1," "1-2," and "2-3" bonds).

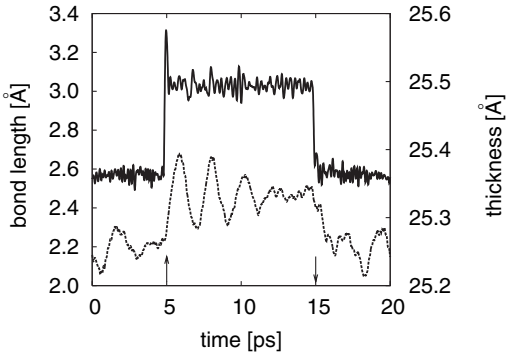

FIG. 3. Atomic distance separation of breaking bond (solid line) and thickness of sample (dotted line) as a function of time. Arrows indicate that at 5 ps an excited electron was created, while at 15 ps it was annihilated.

However, sometimes we also observed the formation of interchain bonds between two twofold C_2-coordinated atoms ($C_{2,0} + C_{2,0} \Rightarrow C_{2,1} + C_{2,1}$).

The bond breaking and interchain bond formation can be understood in terms of a change in the bond strength before and during the excitations. Within the TB representation, the total bond energy of the system can be written as

$$E = 2\sum_{k}^{\text{occ.}} \epsilon_k = 2\sum_{k}^{\text{occ.}} \sum_{i,j,p,q} c_{i,p}^{(k)} c_{j,q}^{(k)} H_{ij}^{pq} = 2\sum_{k}^{\text{occ.}} \sum_{i \neq j} E_{i,j}^{(k)}, \quad (1)$$

where i, j are atom indices, p, q stand for atomic orbitals (s, p_x, p_y, p_z), ϵ_k is the kth eigenvalue of the Hamiltonian matrix (H_{ij}^{pq}), and $c_{i,p}^{(k)}$ and $c_{j,q}^{(k)}$ are the corresponding eigenvectors [15]. Thus, $E_{i,j}^{(k)}$ is the energy contribution of the particular bond between atoms i and j due to the kth eigenstate.

The change in the bond energy due to the excitation of the electron is given by $\Delta E_{\text{bond}} = \epsilon_{\text{LUMO}} = \sum_{i,j} E_{i,j}^{\text{LUMO}}$. Let the indices l and m denote the two atoms where the bond breaking occurs and where the LUMO is mainly localized on the atoms such as "0" in Fig. 2. We found that energies $E_{i \neq l, j \neq m}^{\text{LUMO}}$ are negligibly small compared to the bond-breaking site $E_{l,m}^{\text{LUMO}}$ of 0.43 eV. After bond breaking, the latter decreases to 0.19 eV. This is due to the excited electron occupying an antibonding state during illumination, thereby leading to a decrease in the bonding energy of 0.24 eV.

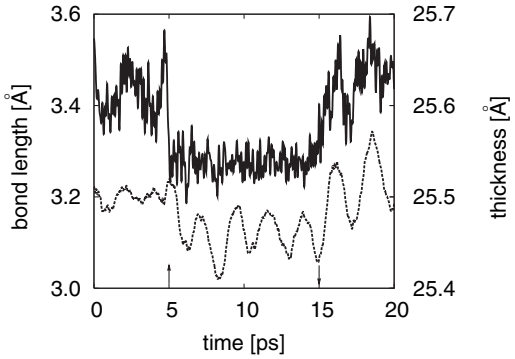

FIG. 4. Atomic distance separation of interchain bond (solid line) and thickness of sample (dotted line) as a function of time. Arrows indicate that at 5 ps a hole was created, while at 15 ps it was annihilated.

In contrast, hole creation leads to a change in the bond energy of $\Delta E_{\text{bond}} = -\epsilon_{\text{HOMO}} = -\sum_{i,j} E_{i,j}^{\text{HOMO}}$. Let the indices f and g label the two atoms where an interchain bond is formed. In a representative sample, $-E_{f,g}^{\text{HOMO}}$ was -0.026 eV before hole creation, changing to -0.068 eV during the interchain bond formation. During illumination, therefore, there is a decrease in occupancy of nonbonding states due to the annihilation of electrons (i.e., hole creation), which leads to an increase in the bonding energy. After removing an electron from a nonbonding orbital (i.e., the lone pairs), the energy is lowered by strengthening the corresponding weak interchain covalent bond.

In order to model the collective effect of photoinduced changes in amorphous selenium, we also performed simulations in which five electrons were excited and five holes created. The five excited electrons were obtained by placing the electrons from the five highest occupied energy levels (one electron from each level) into the five lowest unoccupied energy levels (again, one electron into each level). We found similar effects as described above for the single electron (hole) creation: The bond breaking and interchain bond formation have similar characteristics to those seen in Figs. 2–4. Nevertheless, for the five excited electrons, further bond breaking occurred not only at the C_3 sites but also at some C_2 sites. In the case of the five holes, we observed that interchain bonds were formed between C_1 and C_2 sites and also between C_2 and C_2 sites. Finally, we made several different types of combinations like two, three, four electrons or holes and like two, three, four electrons and holes were in the system. We obtained always the same conclusion. These results confirm that volume expansion and volume shrinkage are additive quantities; namely, the expansion in thickness d_+ is proportional to the number of excited electrons n_e ($d_+ = \bar{\beta}_+ n_e$), while the shrinkage d_- is proportional to the number of created holes n_h ($d_- = \bar{\beta}_- n_h$). The parameter $\bar{\beta}_+$ ($\bar{\beta}_-$) is the average thickness change caused by an excited electron (hole). The time dependent thickness change is equal to $\Delta(t) = d_+(t) - d_-(t) = \bar{\beta}_+ n_e(t) - \bar{\beta}_- n_h(t)$. Assuming $n_e(t) = n_h(t) = n(t)$, we get

$$\Delta(t) = (\bar{\beta}_+ - \bar{\beta}_-) n(t) = \bar{\beta}_\Delta n(t), \quad (2)$$

where $\bar{\beta}_\Delta$ is a characteristic constant of the chalcogenide glass related to photoinduced volume (thickness) change, and it is a unique parameter for each glass. The sign of this parameter governs whether the material shrinks or expands.

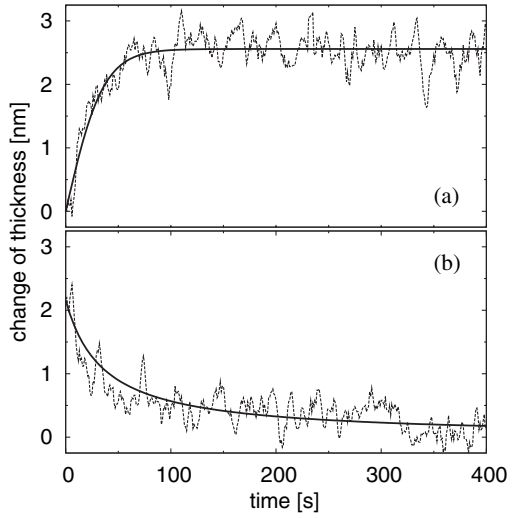

FIG. 5. Measured photoinduced changes in amorphous selenium. Upper panel: expansion due to illumination (dotted line) and fitted $\Delta(t) = \sqrt{\tilde{G}/\tilde{C}}\tanh(\sqrt{\tilde{G}\,\tilde{C}}t)$ curve (solid line). Best fit gives $\tilde{G} = 0.072\ \mathrm{nm\,s^{-1}}$ and $\tilde{C} = 0.011\ \mathrm{nm^{-1}\,s^{-1}}$. Lower panel: shrinkage after switching off illumination (dotted line) and fitted theoretical curve $\Delta(t) = a/(a\tilde{C}t + 1)$ (solid line). Best fit provides $\tilde{C} = 0.013\ \mathrm{nm^{-1}\,s^{-1}}$ and $a = 2.16$ nm.

The number of electrons excited and holes created is proportional to the time during illumination. Their generation rate G depends on the photon absorption coefficient and the number of incoming photons. After photon absorption, the excited electrons and holes migrate within the amorphous sample and then eventually recombine. A phenomenological equation for this dominant process can be written as

$$\frac{dn_e(t)}{dt} = G - Cn_e(t)n_h(t), \tag{3}$$

where C is a constant. Using $n_e(t) = n_h(t) = n(t)$, $\tilde{G} \equiv G\bar{\beta}_\Delta$, and $\tilde{C} \equiv C/\bar{\beta}_\Delta$, we obtain an equation for the time dependent volume change $\Delta(t)$, namely,

$$\frac{d\Delta(t)}{dt} = \tilde{G} - \tilde{C}\Delta^2(t). \tag{4}$$

Solution of this nonlinear differential equation is given by

$$\Delta(t) = \sqrt{\frac{\tilde{G}}{\tilde{C}}}\tanh(\sqrt{\tilde{G}\,\tilde{C}}t). \tag{5}$$

Recently, the photoinduced expansion of amorphous selenium films was measured *in situ* for the first time using optoelectronic interference, enhanced by image precessing [8]. Figure 5(a) shows the measured time evolution of the surface height in the interval of 0–400 s. The best fit according to Eq. (5) gives $\tilde{G} = 0.072\ \mathrm{nm\,s^{-1}}$ and $\tilde{C} = 0.011\ \mathrm{nm^{-1}\,s^{-1}}$, as seen in Fig. 5(a). After the light is turned off, Eq. (4) reduces to $d\Delta(t)/dt = -\tilde{C}\Delta^2(t)$ with the solution $\Delta(t) = a/(a\tilde{C}t + 1)$. Figure 5(b) displays the measured decay and the fitted theoretical curve with $\tilde{C} = 0.013\ \mathrm{nm^{-1}\,s^{-1}}$ and $a = 2.16$ nm. Although the slight difference in the value of $\tilde{C}$ in the above two fits is within the error bar, this discrepancy might be expected because we rarely found irreversible changes in the local atomic arrangements in our TB-MD simulations.

In summary, we have proposed a comprehensive explanation of photoinduced volume changes in chalcogenide glasses. We found covalent bond breaking in systems with excited electrons, whereas holes contribute to the formation of interchain bonds in the vicinity where these excited electrons and holes are localized. The interplay between photoinduced bond breaking and interchain bond formation leads to either volume expansion or shrinkage. Our comprehensive microscopic explanation of the photoinduced volume change is in an excellent agreement with the first *in situ* surface height measurements in amorphous selenium.

This work has been supported by the OTKA Fund (Grants No. T038191 and No. T043231) and by Hungarian-British and Hungarian-Japanese intergovernmental S&T Programmes (No. GB-17/03 and No. JAP-8/02). Simulations have been carried out using computer resources provided us by Tokyo Polytechnic University. We are indebted to Professor Takeshi Aoki for this possibility. We acknowledge valuable discussions with Ralf Drautz at the University of Oxford and with Professor Peter Thomas (Marburg).

[1] Y. Kuzukawa, A. Ganjoo, and K. Shimakawa, J. Non-Cryst. Solids **227–230**, 715 (1998).
[2] K. Shimakawa, N. Yoshida, A. Gahjoo, A. Kuzukawa, and J. Singh, Philos. Mag. Lett. **77**, 153 (1998).
[3] K. Shimakawa, A. Kolobov, and S. R. Elliott, Adv. Phys. **44**, 475 (1995).
[4] H. Fritzsche, Solid State Commun. **99**, 153 (1996).
[5] A. V. Kolobov, H. Oyanagi, K. Tanaka, and Ke. Tanaka, Phys. Rev. B **55**, 726 (1997).
[6] X. Zhang and D. A. Drabold, Phys. Rev. Lett. **83**, 5042 (1999).
[7] V. Palyok, I. A. Szabo, D. L. Beke, and A. Kikineshi, Appl. Phys. A **74**, 683 (2002).
[8] Y. Ikeda and K. Shimakawa, J. Non-Cryst. Solids **338–340**, 539 (2004).
[9] K. Kohary and S. Kugler, Phys. Rev. B **63**, 193404 (2001).
[10] K. Kohary and S. Kugler, Mol. Simul. **30**, 17 (2004).
[11] D. Molina, E. Lomba, and G. Kahl, Phys. Rev. B **60**, 6372 (1999).
[12] E. Lomba, D. Molina, and M. Alvarez, Phys. Rev. B **61**, 9314 (2000).
[13] F. Shimojo, K. Hoshino, and Y. Zempo, J. Phys. Condens. Matter **10**, L177 (1998).
[14] D. Moses, Phys. Rev. B **53**, 4462 (1996).
[15] D. G. Pettifor, *Bonding and Structure of Molecules and Solids* (Oxford Science Publications, Oxford, 1995).